A COMPREHENSIVE FINITE ELEMENT NAVIER-STOKES SOLVER FOR LOW- AND HIGH-SPEED AIRCRAFT DESIGN

Frédéric Chalot†
Division of Applied Mechanics, Stanford University, Stanford, CA 94305-4040, USA

Michel Mallet‡
*Michel Ravachol**
Dassault Aviation, 92214 Saint-Cloud, France

Abstract

Recent developments of a solver for the Navier-Stokes equations using the Finite Element Method are described. They include improved turbulent modeling capabilities using two-equation turbulence models with accurate treatment of the transport terms and boundary conditions. Consistent extensions to chemically reacting air in equilibrium and nonequilibrium using entropy variables are also described. Numerical results illustrate the capability of the method for design calculations.

1. Introduction

A Navier-Stokes Finite Element solver has been developed. This paper will present the more recent additions to the simulation capabilities of the tool and a few examples of three dimensional calculations performed for aerothermal design of aircrafts. Accurate and efficient implementation of turbulence models based on transport equations on unstructured meshes are described. Consistent extension to thermochemical equilibrium and nonequilibrium flows using entropy variables is discussed.

The Navier-Stokes equations including the effects of turbulence are written in section 2 and a review of the Galerkin/least-squares method is presented. In section 3, the turbulence models implementation is discussed with special emphasis on the numerical technique used. In section 4, equilibrium and nonequilibrium thermochemical models are described. Finally numerical results are presented in section 5.

2. Overview of the solver

2.1. Governing equations

Let ρ, $\boldsymbol{u}$, and E be respectively the density, the velocity, and the total energy per unit mass of fluid. The Navier-Stokes equations read:

- conservation of mass

$$\frac{\partial \rho}{\partial t} + \nabla \cdot (\rho \boldsymbol{u}) = 0, \tag{1}$$

- Newton's second law

$$\frac{\partial \rho \boldsymbol{u}}{\partial t} + \nabla \cdot (\rho \boldsymbol{u} \otimes \boldsymbol{u}) = \nabla \cdot \boldsymbol{\sigma}, \tag{2}$$

- conservation of energy

$$\frac{\partial \rho E}{\partial t} + \nabla \cdot (\rho E \boldsymbol{u}) = \nabla \cdot (\boldsymbol{\sigma} \boldsymbol{u}) - \nabla \cdot \boldsymbol{q}, \tag{3}$$

where $\boldsymbol{\sigma}$ is the Cauchy stress tensor and $\boldsymbol{q}$ is the heat-flux vector. This set of partial differential equations is subsidized with appropriate constitutive relations and state equations which we will describe in the following sections. We can notice that up to this point no particular alteration to the usual Navier-Stokes equations is made to accommodate for turbulence and/or high-temperature effects. Thus the strategy developed for the solution of laminar flows of a perfect gas can be formally applied. The numerical method used is discussed in the next section.

2.2. The Galerkin/least-squares formulation

This formulation has developed into a general approach for a wide class of problems. The basic idea can be understood by considering the steady scalar advection-diffusion model problem:

$$\mathcal{L}u = \boldsymbol{a} \cdot \nabla u - \nabla \cdot \boldsymbol{K} \nabla u = \boldsymbol{0}.$$

where $\boldsymbol{a}$ and $\boldsymbol{K}$ are constant parameters. For simplicity we assume that u vanishes on the boundary. The Galerkin method is defined as:

---

† Graduate Research Assistant, on leave at Dassault Aviation
‡ Research Scientist
* Research Scientist, Member AIAA

Find $u^h \in \mathcal{V}^h$ such that for all $w^h \in \mathcal{V}^h$, $B(w^h, u^h) = 0$ where

$$B(w^h, u^h) = \int_\Omega (w^h \boldsymbol{a} \cdot \nabla u^h + \nabla w^h \cdot \boldsymbol{K} \nabla u^h) d\Omega$$

The Galerkin/least-squares method can be defined by the following variational equation:

$$B(w^h, u^h) + \sum_e \int_{\Omega^e} \mathcal{L} w^h \tau \mathcal{L} u^h d\Omega^e = 0$$

The additional term is the sum of integrals over element interior (a finite element discretization of the domain is assumed). It adds stability to the Galerkin formulation without upsetting the consistency of the method. A convergence analysis of this method has been performed.[1] For the multidimensional case, the numerical diffusion is characterized by the diffusivity matrix $\boldsymbol{K}^{\text{num}} = \boldsymbol{a} \tau \boldsymbol{a}^T$ where $\tau = \dfrac{h}{2} \dfrac{f(Pe)}{|\boldsymbol{a}|}$ and $f(Pe) = \coth(Pe) - 1/Pe$ is a doubly asymptotic function of the element Peclet number ($Pe = |\boldsymbol{a}|h/2|\boldsymbol{K}|$) going to zero when diffusion dominates and to one when advection dominates.

The Galerkin/least-squares method can be extended to symmetric linear advective systems. In the case of a system of n equations, $\boldsymbol{\tau}$ is an $n \times n$ symmetric matrix; we can write its eigenvalues decomposition $\boldsymbol{\tau} = \sum_{i=1}^n T_i \tau_i T_i^T$. In the presence of physical diffusion, the matrix $\boldsymbol{\tau}$ is modified; it becomes $\boldsymbol{\tau} = \sum_{i=1}^n T_i f(Pe_i) \tau_i T_i^T$ where Pe_i is the Peclet number corresponding to the i^{th} mode, $Pe_i = \dfrac{h}{2} \dfrac{\tau_i}{K_i}$. The doubly asymptotic behavior is present in each mode in the numerical diffusion. This ingredient of the method is critical in establishing the convergence results presented in Hughes, Franca and Mallet[2] for linear systems of advection-diffusion equations. The formulation can be applied to the compressible Navier-Stokes equations which can be written in the form of a symmetric advective-diffusive system in terms of entropy variables, as we will see shortly.

<u>Entropy variables</u>

We define the generalized entropy function $\mathcal{H}$ by $\mathcal{H} = \mathcal{H}(\boldsymbol{U}) = -\rho s$, where s is the physical entropy per unit mass. $\mathcal{H}$ is a strictly convex function of the vector of conservative variables,

$$\boldsymbol{U} = \frac{1}{v} \left\{ \begin{array}{c} 1 \\ \boldsymbol{u} \\ e + |\boldsymbol{u}|^2/2 \end{array} \right\}$$

where $v = 1/\rho$ is the specific volume. Consequently, the relation $\boldsymbol{V}^T = \partial \mathcal{H} / \partial \boldsymbol{U}$ constitutes a legitimate change of variables. $\boldsymbol{V}$ is referred to as the vector of *(physical) entropy variables*. They were originally derived with the perfect gas case in mind, but were recently extended to take chemistry and high-temperature effects into account.[3] For example, in the case of a general divariant gas such as one describing a flow in thermochemical equilibrium (see section 4), they can be written as

$$\boldsymbol{V} = \frac{1}{T} \left\{ \begin{array}{c} \mu - |\boldsymbol{u}|^2/2 \\ \boldsymbol{u} \\ -1 \end{array} \right\},$$

where $\mu = e + pv - Ts$ is the chemical potential of the considered gas mixture, p and T being respectively the thermodynamic pressure and temperature. Introducing this change of variables, the mean flow equations read:

$$\widetilde{\boldsymbol{A}}_0 \frac{\partial \boldsymbol{V}}{\partial t} + \widetilde{\boldsymbol{A}} \cdot \nabla \boldsymbol{V} = \nabla \cdot (\widetilde{\boldsymbol{K}} \nabla \boldsymbol{V}) \qquad (4)$$

in which

(i) $\widetilde{\boldsymbol{A}}_0$ is symmetric and positive definite;
(ii) the $\widetilde{\boldsymbol{A}}_i$'s are symmetric ($\widetilde{\boldsymbol{A}} = \{\widetilde{\boldsymbol{A}}_i\}$);
(iii) $\widetilde{\boldsymbol{K}}$ is symmetric and positive semi-definite.

We wish to stress the fact that the method is conservative, even though entropy variables are used. When using entropy variables, the weak formulation enforces the Clausius-Duhem inequality, which constitutes a statement of the second law of thermodynamics, on the discrete solution. Numerical solutions are actually carried out in terms of entropy variables.

<u>Discontinuity capturing operator</u>

Although the Galerkin/least-squares method is a stable method, oscillations may occur in the vicinity of strong gradients. A nonlinear discontinuity-capturing operator is added to the formulation. It is defined elementwise as:

$$\int_{\Omega^e} \nu^h \left(\mathcal{L}(\boldsymbol{V}^h) \right) \nabla_{\boldsymbol{\xi}} \boldsymbol{W}^h \cdot \widetilde{\boldsymbol{A}}_0 \nabla_{\boldsymbol{\xi}} \boldsymbol{V}^h \, d\Omega$$

where $\nabla_{\boldsymbol{\xi}}$ is the gradient in the element local coordinate system. Various definitions of ν^h have been proposed including linear and quadratic versions.[4]

<u>Implicit iterative time-marching algorithm</u>

Convergence to steady-state of the compressible Navier-Stokes equations is achieved through an implicit iterative time-marching algorithm. At each discrete time t_n, the finite element discretization leads to the following nonlinear problem:

Given the solution vector $\boldsymbol{v}_{(n-1)}$ *at time* t_{n-1}*, and a time increment* Δt*, find the solution vector* $\boldsymbol{v}$ *at time* t_n*, which satisfies the nonlinear system of equations*

$$\boldsymbol{G}(\boldsymbol{v};\boldsymbol{v}_{(n-1)},\Delta t)=\boldsymbol{0} \tag{5}$$

$\boldsymbol{G}$ is a system of nonlinear functionals of $\boldsymbol{v}$ and of parameters $\boldsymbol{v}_{(n-1)}$ and Δt. This system is solved for $\boldsymbol{v}$ by performing a linearization through a truncated Taylor series expansion of $\boldsymbol{G}$. This leads to a linear nonsymmetric system of equations of the form

$$\boldsymbol{J}\,\boldsymbol{p}=-\boldsymbol{R}$$

where

$$\boldsymbol{J}=\frac{\partial\boldsymbol{G}}{\partial\boldsymbol{v}}(\boldsymbol{v}_{(n-1)};\boldsymbol{v}_{(n-1)},\Delta t) \tag{6}$$

$$\boldsymbol{p}\overset{\text{def}}{=}\boldsymbol{v}-\boldsymbol{v}_{(n-1)} \tag{7}$$

$$\boldsymbol{R}=\boldsymbol{G}(\boldsymbol{v}_{(n-1)};\boldsymbol{v}_{(n-1)},\Delta t) \tag{8}$$

$\boldsymbol{R}$ is the residual of the nonlinear problem and $\boldsymbol{J}$ is the consistent Jacobian associated with $\boldsymbol{R}$. The consistent Jacobian is often replaced by a Jacobian-like matrix $\mathcal{J}$ leading to a more stable time-marching algorithm.[5] A residual-like vector $\mathcal{R}$ associated with $\mathcal{J}$ can be defined as

$$\mathcal{J}\overset{\text{def}}{=}\frac{\partial\mathcal{R}}{\partial\boldsymbol{v}}$$

The system of equations $\mathcal{J}\,\boldsymbol{p}=-\boldsymbol{R}$ is preconditioned by a nodal block-diagonal preconditioner[6] and solved using the Generalized Minimal RESidual (GMRES) algorithm introduced by Saad and Schultz.[7]

3. Turbulent flow modeling using transport equations

3.1. Closure assumptions

The partial differential equations used to describe the mean flow field are the mass-averaged Navier-Stokes equations of a compressible fluid. The closure of the Reynolds stress tensor and heat flux is obtained using a classical Boussinesq hypothesis and the concept of eddy viscosity. The eddy viscosity is computed through a two-equation turbulence model, thus the Navier-Stokes equations are augmented by two additional partial differential equations for the turbulence quantities. Modeling constants are necessary in both of these equations for closure.

The only change encountered by the Navier-Stokes equations written in mass-average form is the new definition of the Cauchy stress tensor $\boldsymbol{\sigma}$, the total energy E, and the heat flux vector $\boldsymbol{q}$ which now read:

$$\begin{aligned}\boldsymbol{\sigma}&=(\mu^{\text{visc}}+\mu_t^{\text{visc}})\{\nabla\boldsymbol{u}+\nabla\boldsymbol{u}^T-\frac{2}{3}\nabla\cdot\boldsymbol{u}\boldsymbol{1}\}\\&\quad-(p+\frac{2}{3}\rho k)\boldsymbol{1},\\E&=e+\frac{1}{2}|\boldsymbol{u}|^2+k,\\\boldsymbol{q}&=-(\kappa+\kappa_t)\nabla T.\end{aligned}$$

The molecular viscosity is μ^{visc}; μ_t^{visc} is the eddy viscosity; k is the turbulent kinetic energy; κ and κ_t are respectively the laminar and turbulent coefficient of thermal conductivity; the laminar Prandtl number is taken as $P_r=\mu^{\text{visc}}c_p/\kappa=0.72$ and the turbulent Prandtl number is taken as $P_{rt}=\mu_t^{\text{visc}}c_p/\kappa_t=0.9$, where c_p is the specific heat at constant pressure. The internal energy e and the equation of state are defined according to the chosen thermodynamic model.

3.2. Turbulence Model

The turbulence models used belong to the $k-\epsilon$ family.[8] The extra equations which are needed can be written as

$$\rho\frac{\partial s_i}{\partial t}+\rho\boldsymbol{u}\cdot\nabla s_i-\nabla\cdot\left((\mu^{\text{visc}}+\frac{\mu_t^{\text{visc}}}{\sigma_i})\nabla s_i\right)=H_i.$$

In the case of the classical $k-\epsilon$ turbulence model the variables are $s_1=k$ and $s_2=\epsilon$. The eddy viscosity is then defined as

$$\mu_t^{\text{visc}}=\rho C_\mu\frac{k^2}{\epsilon}.$$

These equations are convection-diffusion equations mainly coupled through their source terms. The turbulence quantities are positive, therefore one is seeking a scheme which enforces this constraint. This can be achieved through the use of a monotone discrete advective operator.

Another difficulty arising in the use of transport equations turbulence models lies in the treatment of the boundary conditions. Two main strategies can be utilized, one can either modelize the viscous sublayer by suitable law of the wall or one can integrate the Navier-Stokes equations and the turbulence equations through the viscous sublayer. This point will be addressed later.

3.3. Monotone Scheme for the turbulence equations

The positivity of the turbulence variables is achieved by the combination of two main features : the use of a monotone advective scheme and the time discretization of the source term.

First we will investigate the issue of the spatial discretization scheme. The basic choice to enforce the monotony of the discrete advection diffusion equation would be to used a first order upwind scheme. In so doing, even on a simple advection diffusion equation, the sharp gradient are completely smeared out as illustrated in figure 1. It is thus necessary to implement a scheme of higher accuracy. The scheme chosen is the one advocated by Deconinck and Roe.[9] The main advantages of the scheme, along with its monotonicity and its low diffusion, are its compact stencil and the fact that all the necessary evaluations are performed element by element yielding an easy implementation in a Finite Element framework as well as a straightforward vectorization. The efficiency of the scheme is illustrated on the same advection-diffusion test problem solved with the first order scheme (figure 2). Such an elaborate treatment is needed in order to calibrate the accuracy of the modeling of the turbulent effects. With too coarse a numerical treatment such as a first order upwinding it is impossible to analyze the validity of any turbulence model.

3.4. Time discretization for the turbulence equations

For the $k-\epsilon$ model the source terms read

$$H_k = \mu_t^{\text{visc}} P - \frac{2}{3}\rho k S - \rho\epsilon,$$

and

$$H_\epsilon = C_1 \frac{\epsilon}{k}\mu_t^{\text{visc}} P - \frac{2}{3} C_1 \epsilon S - \rho C_2 \frac{\epsilon^2}{k}.$$

It is clear that the source terms can be written as $H_i = H_i^+ - H_i^-$, with both terms positive. Then the time discretization applies as follow H_i^+ is treated explicitly and H_i^- semi-implicitly. The final time discretization for the $k-\epsilon$ model is

$$\begin{aligned}\rho^n(\frac{1}{\Delta t} + \frac{\epsilon^n}{k^n})k^{n+1} &+ \rho^n \boldsymbol{u}^n \cdot \nabla k^{n+1} \\ &- \nabla \cdot \left((\mu^{\text{visc}} + \frac{{\mu_t^{\text{visc}}}^n}{\sigma_k}) \nabla k^{n+1} \right) \\ &= \frac{\rho^n}{\Delta t} k^n + P^n,\end{aligned}$$

$$\begin{aligned}\rho^n(\frac{1}{\Delta t} + C_2\frac{\epsilon^n}{k^n})\epsilon^{n+1} &+ \rho^n \boldsymbol{u}^n \cdot \nabla \epsilon^{n+1} \\ &- \nabla \cdot \left((\mu^{\text{visc}} + \frac{{\mu_t^{\text{visc}}}^n}{\sigma_\epsilon}) \nabla \epsilon^{n+1} \right) \\ &= \frac{\rho^n}{\Delta t}\epsilon^n + C_1\frac{\epsilon^n}{k^n} P^n,\end{aligned}$$

The terms P and S are given by

$$P = (\nabla \boldsymbol{u} + \nabla \boldsymbol{u}^T) : \nabla \boldsymbol{u} - \frac{2}{3}(\nabla \cdot \boldsymbol{u})^2.$$

$$S = \nabla \cdot \boldsymbol{u}$$

The modeling constants have their usual values: $\sigma_k = 1.0$, $\sigma_\epsilon = 1.3$, $C_1 = 1.44$, $C_2 = 1.92$,

3.5. Coupling with the Navier-Stokes equations

The discretized mean flow equations and the turbulence equations are integrated using a splitting method. At a current time step, we solve the Navier-Stokes equations using turbulence data evaluated at the previous time while the turbulence equations are solved using the flow variables computed at the previous time.

3.6. Modeling in the vicinity of a solid boundary

The above turbulence transport equations, for the $k-\epsilon$ model are derived under the hypothesis of a large Reynolds number. Thus, in region close to the wall, such as in the viscous sublayer where molecular effects become important, these equations are not valid. Two approaches have been developed: one is based on a law of the wall and the other uses a two-layer model.

In order to avoid integrating the turbulence equations in these regions we make use of wall functions.[10] Then, the equations for the mean flow and for the turbulence variables are integrated up to a distance $y = y_w$ away from the wall. In the region between the actual wall and the limit of the computational domain $0 < y < y_w$ the flow is assumed to follow a law of the wall

$$\frac{u}{u_\tau} = f\left(\frac{\rho u_\tau y}{\mu^{\text{visc}}}\right)$$

The function f splits the wall layer into three parts and degenerates consistently with a no-slip boundary condition if the mesh happens to be fine enough.

At each time step an estimate of the velocity u at $y = y_w$ can be obtained, then the value of the wall shear stress u_τ is computed from the law of the wall (using a Newton method) and this value is used to get Dirichlet boundary conditions for k and ϵ at the wall. In practice the point $y = y_w$ is close enough to the wall to actually be considered laying on the wall and the boundary conditions may be imposed on the wall surface. For the mean flow equation this results of course in a wall slip boundary condition.

To integrate the equation down to the wall a two-layer model is used. This model has been introduced by Chen and Patel[11] and modifies the k equation in the near wall region while the ϵ equation is replaced by an algebraic definition of the dissipation ϵ, away from the wall the standard $k-\epsilon$ equations are conserved. We thus use two different turbulence models depending on the location with respect to a solid wall. In the wall region we have a one-equation model

$$\rho\frac{\partial k}{\partial t} + \rho\boldsymbol{u}\cdot\nabla k - \nabla\cdot\left((\mu^{\text{visc}} + \frac{\mu_t^{\text{visc}}}{\sigma_k})\nabla k\right) = \mu_t^{\text{visc}}P - \frac{2}{3}\rho k S - \rho\epsilon,$$

and in this case the eddy viscosity is evaluated by

$$\mu_t^{\text{visc}} = \rho C_\mu \sqrt{k} l_\mu,$$

with

$$l_\mu = Cy\left(1 - \exp(-R_y/A)\right);$$

and ϵ is computed as follows

$$\epsilon = \frac{k^{3/2}}{l_\epsilon}$$

with

$$l_\epsilon = Cy\left(1 - \exp(-R_y/A_2)\right).$$

with

$$R_y = \frac{\rho\sqrt{k}y}{\mu^{\text{visc}}}$$

where y is the distance to the wall. The blending between the two models is performed at $R_y = 150$, which corresponds to $y^+ = 80$ which is well within the logarithmic region.

Since the Navier-Stokes equations are integrated down to the wall, separation can be accurately computed. Moreover, the mesh needs to be fine enough to allow accurate computation of the wall layer ($y^+ \leq 10$).

4. Thermochemical models

4.1. Thermochemical equilibrium

The very high Mach number flows associated with hypersonic reentry flight involve strong shock waves. Upstream of the bow shock, the temperature is low and air is a uniform mixture. Through the shock, the temperature increases, vibrational modes are excited, and dissociation takes place. Since dissociation reactions are endothermic, the temperature rise tends to be limited. In a first step, the equilibrium hypothesis can be made: it assumes that the chemical characteristic time scale is much smaller than that of the fluid flow. Typically, flow solvers must be modified so that at each time step, the state equation takes into account the local state of equilibrium.

In the present paper, air is considered as a mixture of five species: N_2, O_2, NO, N, and O. In our case, the thermodynamic state of the system is defined by the entropy variables, viz., the chemical potential of the mixture μ and the temperature T. Given this two quantities, we need to solve for the partial pressures p_s of the 5 considered species. Consequently we need a set of 5 equations. Two of these are provided first by writing the chemical potential as a function of the p_s's and T, and secondly by stating that the local proportion of oxygen atoms relative to nitrogen atoms is constant:

$$\sum_s y_s(p_s)\mu_s(p_s,T) = \mu \tag{9}$$

$$\frac{2p_{\text{N}_2} + p_{\text{NO}} + p_{\text{N}}}{2p_{\text{O}_2} + p_{\text{NO}} + p_{\text{O}}} = \frac{79}{21} \tag{10}$$

where y_s is the mass fraction of species s. It is given in terms of the partial pressures as

$$y_s = \frac{\hat{M}_s}{\hat{M}}x_s. \tag{11}$$

In turn, x_s, the mole fraction of species s, and $\hat{M}$, the molar mass of the mixture, are given in terms of the partial pressures and of the molar masses $\hat{M}_s$ of the different species by

$$x_s = \frac{p_s}{p} \quad , \quad \hat{M} = \sum_s x_s\hat{M}_s. \tag{12}$$

The pressure is provided by Dalton's law of partial pressures:

$$p = \sum_s p_s. \tag{13}$$

The chemical potential of species s, μ_s, is related to the molar chemical potential of the same species, $\hat{\mu}_s$, by

$$\hat{\mu}_s = \mu_s\hat{M}_s = \hat{\mu}_s^0(T) + \hat{R}T\ln p_s \tag{14}$$

where $\hat{R} = 8.31441$ J/mol.K is the universal gas constant, and $\hat{\mu}_s^0$ is the molar chemical potential of species s in the pure state and at unit pressure. It is assumed here that $\hat{\mu}_s^0$ is that of a thermally perfect gas. The corresponding expression can be found in Chalot and Hughes.[12] Particular care must be taken in computing the absolute entropy whose reference value is provided by statistical mechanics.

Three extra equations are needed: law of mass action can be written for three independent chemical reactions. For consistency, we do not state the equilibrium condition for reaction R in the usual form, i.e.,

$$\prod_s p_s^{\nu_{sR}} = K_{pR}(T) \tag{15}$$

where ν_{sR} is the stoichiometric coefficient of species s in reaction R, and $K_{pR}(T)$ the equilibrium constant of reaction R. The latter is a function of temperature which is often given in the form of a curve fit of experimental results. In lieu, we write for each reaction the following statement which is equivalent to (15) , but does not require any extraneous data:

$$\sum_s \nu_{sR}\hat{\mu}_s = 0. \tag{16}$$

Once a model has been chosen for the internal energies of the different species, the system is self-sufficient, and the addition of any extra data, such as equilibrium constants, can only introduce inconsistencies. For the 5 species model considered here, these equations read:

$$\hat{\mu}_{\mathrm{N}_2} = 2\hat{\mu}_{\mathrm{N}} \tag{17}$$

$$\hat{\mu}_{\mathrm{O}_2} = 2\hat{\mu}_{\mathrm{O}} \tag{18}$$

$$\hat{\mu}_{\mathrm{NO}} = \hat{\mu}_{\mathrm{N}} + \hat{\mu}_{\mathrm{O}}. \tag{19}$$

The above set of 5 algebraic equations is solved using Newton method. An initial guess for the 5 partial pressures is obtained from a table look-up, so that convergence of the Newton process is reached in 2 iterations. The last Newton Jacobian matrix provides the necessary derivatives to construct the matrices $\widetilde{\boldsymbol{A}}_0$ and $\widetilde{\boldsymbol{A}}_i$'s.[12]

4.2. Thermochemical nonequilibrium

We present here the extension of the solver described above to thermochemical nonequilibrium. We still consider air as a mixture of the five species N_2, O_2, NO, N, and O, interacting in any number of finite rate chemical reactions. At this stage, the vibrational degrees of freedom of all molecules are represented by a single temperature T^{vib} which can be in or out of equilibrium with the trans-rotational temperature T.

The Navier-Stokes equations (1) –(3) are replaced by the following set of equations:

- <u>species conservation of mass</u>

$$\frac{\partial \rho_s}{\partial t} + \nabla\cdot(\rho_s \boldsymbol{u}) + \nabla\cdot \boldsymbol{J}_s = \Omega_s \qquad s = 1,\ldots,5, \tag{20}$$

- <u>Newton's second law</u>

$$\frac{\partial \rho \boldsymbol{u}}{\partial t} + \nabla\cdot(\rho\boldsymbol{u}\otimes\boldsymbol{u}) = \nabla\cdot\boldsymbol{\sigma}, \tag{21}$$

- <u>conservation of energy</u>

$$\frac{\partial \rho E}{\partial t} + \nabla\cdot(\rho E\boldsymbol{u}) + \nabla\cdot(\boldsymbol{J}\boldsymbol{h}) = \nabla\cdot(\boldsymbol{\sigma}\boldsymbol{u}) - \nabla\cdot\boldsymbol{q} - \nabla\cdot\boldsymbol{q}^{\mathrm{vib}}, \tag{22}$$

- <u>conservation of vibrational energy</u>

$$\begin{aligned}\frac{\partial \rho e^{\mathrm{vib}}}{\partial t} &+ \nabla\cdot(\rho e^{\mathrm{vib}}\boldsymbol{u}) + \nabla\cdot(\boldsymbol{J}\boldsymbol{e}^{\mathrm{vib}}) \\ &= -\nabla\cdot\boldsymbol{q}^{\mathrm{vib}} + \boldsymbol{\Omega}\cdot\boldsymbol{e}^{\mathrm{vib}} + Q^{T-T^{\mathrm{vib}}}. \end{aligned}\tag{23}$$

$\boldsymbol{J} = [J_{si}]^T = [\rho_s v_{si}]^T$ is the mass diffusion matrix, where v_{si} is the diffusion velocity of species s in direction i; $\boldsymbol{h}$ and $\boldsymbol{e}^{\mathrm{vib}}$ are respectively the enthalpy and vibrational energy vectors, $\boldsymbol{h} = \{h_s\}$ and $\boldsymbol{e}^{\mathrm{vib}} = \{e_s^{\mathrm{vib}}\}$; $\boldsymbol{q}$ and $\boldsymbol{q}^{\mathrm{vib}}$ are the heat flux vectors, respectively due to gradients in the translational-rotational temperature T and the vibrational temperature T^{vib}; $\boldsymbol{\Omega}$ is the vector of the production rates of the different species, $\boldsymbol{\Omega} = \{\Omega_s\}$; and $Q^{T-T^{\mathrm{vib}}}$ is the translation-vibration energy transfer rate.

Without any particular assumption on the expressions for the different energies (except that they be functions of the temperatures only), the entropy variables can be derived to be:

$$\boldsymbol{V} = \frac{1}{T}\left\{\begin{matrix} \boldsymbol{\mu} - \dfrac{|\boldsymbol{u}|^2}{2}\boldsymbol{1}_n \\ \boldsymbol{u} \\ -1 \\ 1 - \dfrac{T}{T^{\mathrm{vib}}} \end{matrix}\right\} \tag{24}$$

where $\boldsymbol{\mu} = \{\mu_s\}$ is the vector of chemical potentials, and $\boldsymbol{1}_n^T = \{\underbrace{1,\ldots,1}_{n \text{ terms}}\}$. In the present work the rigid-rotator and harmonic-oscillator model together with the perfect gas assumption were adopted as the equations of state.

Entropy variables appear at their best in this thermochemical context. Each energy conservation equation is replaced by an equation describing the evolution of a quantity trivially related to the different temperatures: there is no need of Newton-type iterations at the end of each time step to extract the temperatures from the energies and to compute the chemical reaction rates, the transport coefficients, and other physical quantities given in terms of temperatures.

In order to satisfy the symmetry requirements, transport phenomena must be modeled using the complete multi-component approach. In this context it is interesting to see how the preservation of symmetry and the respect of the second law of thermodynamics condition the form of constitutive relations to rigorous expressions derived by statistical mechanics means. In particular, the diffusion velocities are given by

$$J_{si} = \rho_s v_{si} = \sum_r \rho \frac{\hat{M}_s \hat{M}_r}{\hat{M}^2} D_{sr} d_{ri} \tag{25}$$

where

$$d_{si} = x_{s,i} + (x_s - y_s)(\ln p)_{,i} \tag{26}$$

where the D_{sr}'s are the multicomponent diffusion coefficients. From the viscosity coefficients of the pure gases the viscosity coefficient of the mixture is computed using Wilke's mixing rule. Species heat conduction coefficients are derived using a modified Eucken formula and are mixed in a fashion which ensures continuity in the thermodynamic equilibrium limit.

The chemical production rate is computed in the usual way[13] and does not take into account any vibration-dissociation coupling yet. The vibrational source term is composed of two parts $\boldsymbol{\Omega} \cdot \boldsymbol{e}^{\text{vib}}$ and $Q^{T-T^{\text{vib}}}$. The first one expresses the fact that molecules disappear or are created with the mean flow vibrational energy ignoring the preferential removal from the higher energy levels. The second one controls the equilibration of vibration with translation. It takes the usual Landau-Teller form where the vibrational relaxation time is computed with the classical semi-empirical formula developed by Millikan and White.

5. Numerical results

Calculation on the RAE2822 transonic airfoil illustrates the accuracy of the solver. The computed case is characterized by $M_\infty = 0.75$, $Re = 6.2 \times 10^6$ and $\alpha = 3.19°$. The computation has been carried out using the law of the wall. Figure 3 shows the iso-Mach lines, figure 4 shows the pressure coefficient on the airfoil and figure 5 shows the skin friction coefficient. Results compare very well with the experimental data.[14]

Calculation of the flow over the canopy of Hermes is presented next. It was performed at the most critical point on the reentry flight path for the windshield design: the altitude is 60 km, the Mach number is 20 and the angle of attack is 30 degrees. At this altitude the Re/m is 120,890. The equilibrium real gas hypothesis was used along with radiative boundary conditions. The mesh includes approximately one million elements. The surface mesh is presented in Figure 6. The finite element approach allows mesh refinement and a precise representation of the details of the geometry in the windshield area. Considerable mesh density is used in the direction perpendicular to the wall. Skin friction lines are presented in Figure 7, complex flow structure is observed. Detailed discussion of Navier-Stokes calculations related to the aerothermal design of Hermes can be found in Naïm *et al.*[15]

The nonequilibrium capability is demonstrated by the simple test case of an inviscid Mach 17.9 flow at zero angle of attack past a circular cylinder with a 10 cm nose radius and extended by 15° planes. The free stream density and temperature are respectively 10^{-4} kg/m^{3}and 231 K. A similar test case is described by Desideri et al.[16] The mesh, pressure, temperature and NO-mass-fraction contours are presented in figures 8–11. The equilibrium and nonequilibrium solutions are displayed respectively in the top and bottom parts. Comparison between perfect gas and equilibrium solutions can be found in previous work.[12]

Conclusion

New extensions to a Navier-Stokes solver have been presented. This solver provides a basis for complex flow simulations dealing with chemistry (equilibrium/ nonequilibrium hypersonic flows) or turbulence. Further developments are underway to propose and test better turbulence models; to improve the modeling of nonequilibrium effects in the flow and provide detailed descriptions of the boundary layer and wall phenomena; to accelerate convergence. It should finally be emphasized that the solver can be implemented with high efficiency on massively parallel machines along the lines of Johan *et al.*,[17] which leads to unprecedented usefulness of the method for design purposes and opens the way to the simulation of ever more challenging flow problems.

Acknowledgements

The authors would like to take the opportunity given here to thank T.J.R. Hughes, Z. Johan, C. Kasbarian, O. Lebigre, M.P. Leclercq, B. Mantel, B. Mohamadi, A. Naïm, J. Périaux, P. Perrier, O. Pironneau,

F. Shakib, and B. Stoufflet for fruitful discussions. The support of DRET, CNES and ESA under R&D grants is acknowledged.

References

[1] C. Johnson, "Streamline Diffusion Methods for problems in Fluid Mechanics," R.H. Gallager et al (eds), Finite Elements in Fluids, Vol. VI, Wiley, London, pp. 251–261, 1986.

[2] T.J.R Hughes, L.P. Franca and M. Mallet, "A New Finite Element Formulation For Computational Fluid Dynamics: VI convergence analysis of the generalized SUPG formulation for linear time dependent multidimensional advective diffusive systems," *Computer Methods in Applied Mechanics and Engineering*, vol. 63, pp. 97–112, 1987.

[3] F. Chalot, T.J.R. Hughes, and F. Shakib, "Symmetrization of conservation laws with entropy for high-temperature hypersonic computations," *Computing Systems in Engineering*, vol. 1, pp. 465–521, 1990.

[4] T.J.R Hughes, M. Mallet and A. Mizukami, "A New Finite Element Formulation For Computational Fluid Dynamics: II beyond SUPG," *Computer Methods in Applied Mechanics and Engineering*, vol. 54, pp. 341–355, 1986.

[5] Z. Johan, T.J.R. Hughes and F. Shakib, "A globally convergent matrix-free algorithm for implicit time-marching schemes arising in finite element analysis in fluids," *Computer Methods in Applied Mechanics and Engineering*, vol. 87, pp. 281–304, 1991.

[6] F. Shakib, T.J.R. Hughes and Z. Johan, "A multi-element group preconditioned GMRES algorithm for nonsymmetric systems arising in finite element analysis," *Computer Methods in Applied Mechanics and Engineering*, vol. 75, pp. 415–456, 1989.

[7] Y. Saad and M.H. Schultz, "GMRES: A generalized minimal residual algorithm for solving nonsymmetric linear systems," *SIAM Journal of Scientific and Statistical Computing*, vol. 7, pp. 856–869, 1986.

[8] B.E. Launder, D.B. Spalding, "The Numerical Computation of Turbulent Flows," *Computer Methods in Applied Mechanics and Engineering*, vol. 3, pp. 269–289, 1974.

[9] R. Struijs, P.L. Roe and H. Deconinck, "Fluctuations Splitting Schemes for the 2D Euler Equations," Von Karman Institute Report, 1991-11/AR.

[10] J.R. Viegas, M.W. Rubesin and C.C Horstman, "On the use of wall functions as boundary conditions for two-dimensional separated compressible flows," AIAA paper 85-0180, 1985.

[11] V.C Patel and H.C. Chen, "Near-wall turbulence models for complex flows including separation," AIAA Journal vol. 29, num. 6.

[12] F. Chalot and T.J.R. Hughes, "A consistent equilibrium chemistry algorithm for hypersonic flows," *Computer Methods in Applied Mechanics and Engineering*, to appear.

[13] C. Park, *Nonequilibrium Hypersonic Aerothermodynamics*, Wiley-Interscience, 1990.

[14] T.L. Holst, "Viscous Transonic Airfoil Workshop. Compendium of Results," AIAA Paper 87-1460, Honolulu 1987.

[15] A. Naïm, M. Mallet, Ph. Rostand, and J.M. Hasholder, "Local aerothermal problems during Hermes reentry," *Theoretical and Experimental Methods in Hypersonic Flows*, AGARD Conference Proceedings 514, pp. 42-1–42-16, 1993.

[16] J.A. Désidéri, N. Glinski, and E. Hettena, "Hypersonic reactive flow computations," *Computers and Fluids*, vol. 18, pp. 151–182, 1990.

[17] Z. Johan, K.K. Mathur, S.L. Johnsson, and T.J.R. Hughes, "An efficient communication strategy for finite element methods on the Connection Machine CM-5 system," *Computer Methods in Applied Mechanics and Engineering*, to appear.

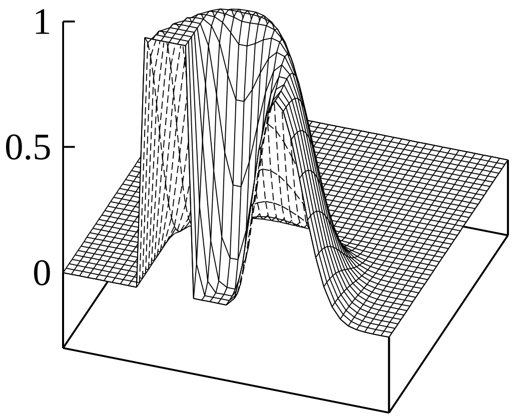

Figure 1. First order upwinding

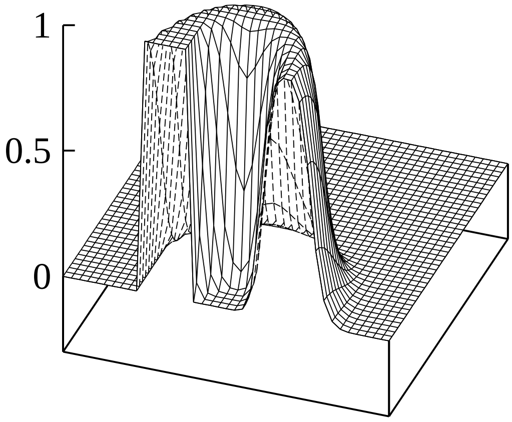

Figure 2. Roe-Deconinck scheme

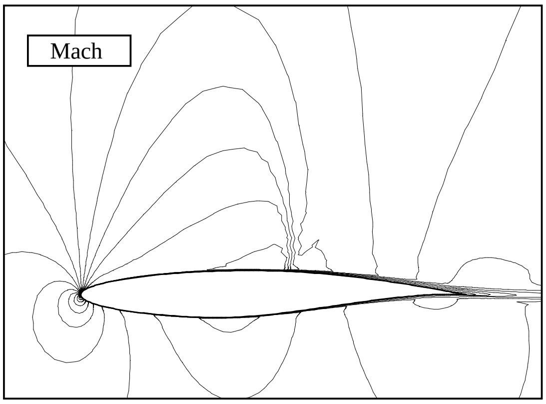

Figure 3. $RAE2822$: $M_\infty = 0.75$, $\alpha = 3.19°$, iso-mach lines

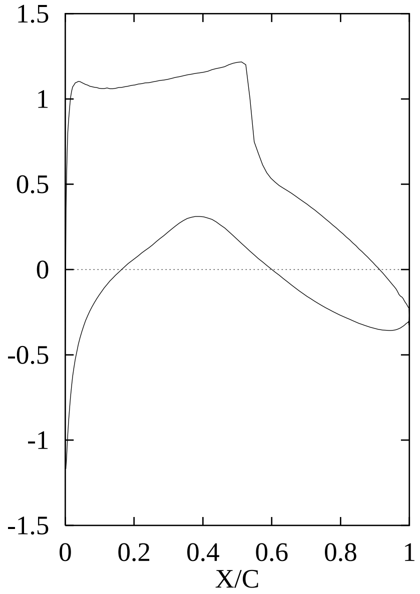

Figure 4. Pressure coefficient $(-C_p)$

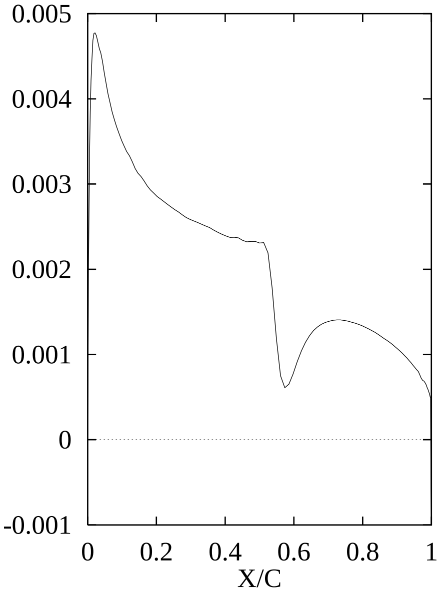

Figure 5. Skin friction coefficient (C_f)

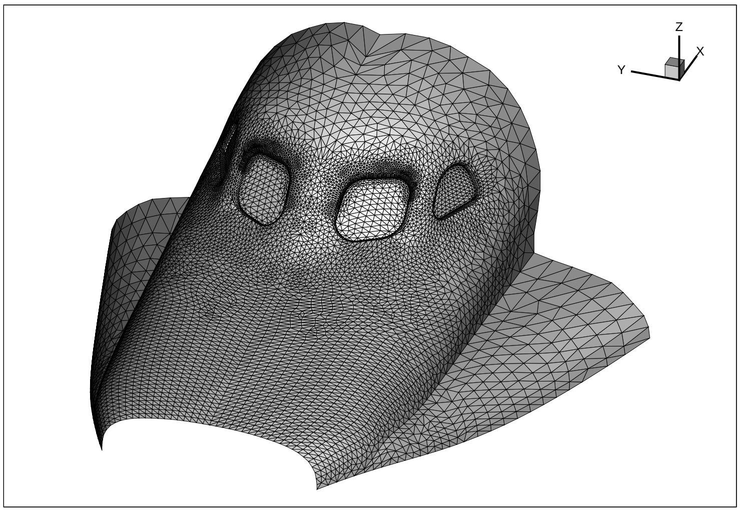

Figure 6. Mesh of the canopy region of the Hermes spaceplane

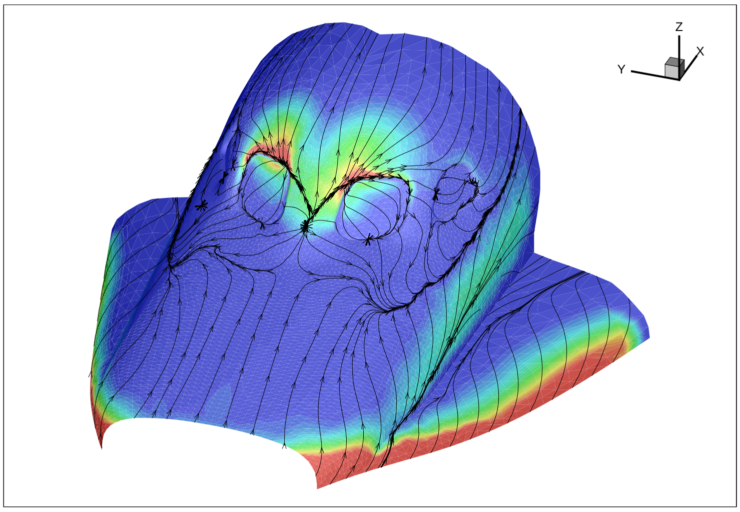

Figure 7. Skin friction lines

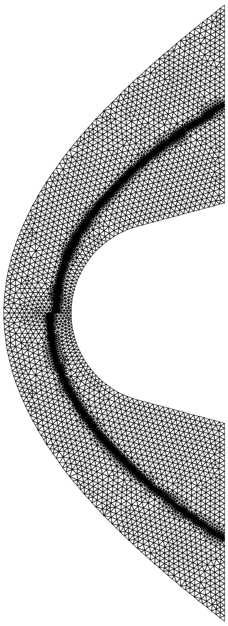

Figure 8. Flow past a blunt body: Mesh

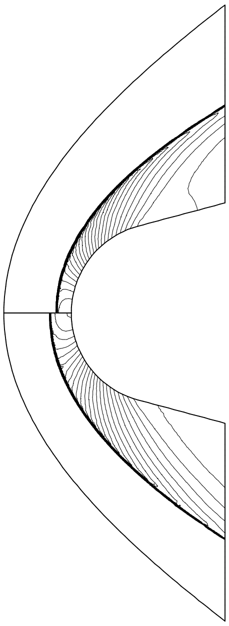

Figure 9. Flow past a blunt body: Pressure contours

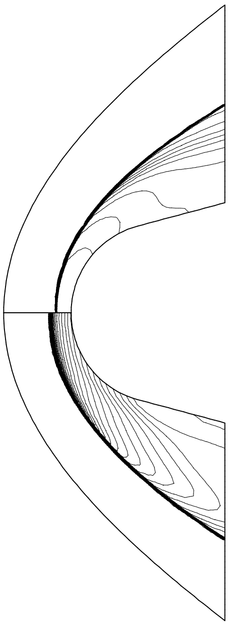

Figure 10. Flow past a blunt body:
Temperature contours

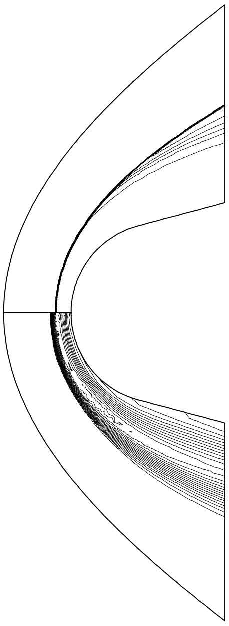

Figure 11. Flow past a blunt body:
NO mass-fraction contours